Weathering without realizing inorganic CO_2 removal revealed through base cation monitoring.

Arthur Vienne[1] , Patrick Frings[2] , Jet Rijnders[1] , Lucilla Boito[1], Jens Hartmann[3] , Harun Niron[1], Reinaldy P. Poetra[3], Miguel Portillo Estrada[1], Tom Reershemius[6], Laura Steinwidder[1], Tim Jesper Suhrhoff[4,5], Sara Vicca[1]

1Biobased Sustainability Engineering (SUSTAIN), Department of Bioscience Engineering, University of Antwerp, Antwerp, Belgium
2 GFZ German Research Centre for Geosciences, Section Earth Surface Geochemistry, Telegrafenberg, 14473 Potsdam, Germany
3 Institute for Geology, Centre for Earth System Research and Sustainability (CEN), Universität Hamburg, Bundesstraße 55, 20146 Hamburg, Germany
4 Yale Center for Natural Carbon Capture, Yale University, New Haven, CT 06511, USA
5 Department of Earth and Planetary Sciences, Yale University, New Haven, CT 06511, USA
6 School of Natural and Environmental Sciences, Newcastle University, Newcastle upon Tyne, UK

Correspondence to: arthur.vienne@uantwerpen.be ; sara.vicca@uantwerpen.be

Keywords: CDR, Enhanced weathering, Monitoring reporting and verification (MRV), sequential extractions, weathering, basalt, time lags for CO2 removal, secondary minerals

Graphical abstract

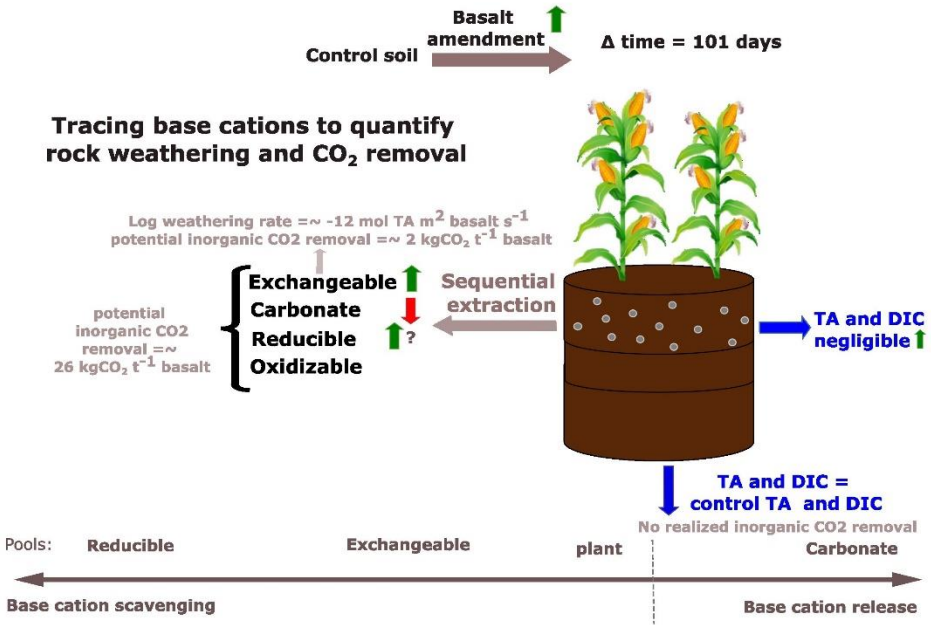

Abstract

Enhanced Weathering using basalt rock dust is a scalable carbon dioxide removal (CDR) technique, but quantifying rock weathering and CDR rates poses a critical challenge. Here, we investigated realized inorganic CO_2 removal (defined as the sum of the change in dissolved inorganic C leaching and in solid inorganic C) and weathering rates by treating mesocosms planted with maize with basalt (0, 10, 30, 50, 75, 100, 150 and 200 t ha^{-1}) and monitoring them for 101 days. We observed no significant realized inorganic CO_2 removal, as leaching of dissolved inorganic carbon did not increase, and soil carbonate content declined over time.

To gain insights into the weathering processes, we traced the fate of base cations in the soil and plants. This analysis showed that most base cations were retained in the topsoil reducible soil pool, typically associated with iron (hydr)oxides, while increases in the exchangeable pool were about a factor 10 smaller. Soil base cation scavenging exceeded plant scavenging by approximately two orders of magnitude. From the base cations in all pools (soil, soil water and plants), we quantified log weathering rates of -11 mol total alkalinity m^{-2} basalt s^{-1}. The

potential inorganic CO_2 removal, defined as the maximum inorganic CO_2 removal achievable if all weathered base cations, adsorbed by soil pools in this experiment, would leach out of the soil and be fully balanced by carbonate anions, was estimated at 26 kg CO_2 t^{-1} basalt.

In conclusion, despite clear weathering of basalt rock, we found no inorganic CO_2 removal within the timescale of this experiment. The observed increase of aluminum in association with the reducible soil fraction indicate the formation of secondary minerals. These, along with enhanced base cation exchange, may contribute to long-term soil fertility and promote the stabilization of soil organic matter.

1. Introduction

To meet the "well below 2°C warming" target established by the United Nations' Paris Agreement, Carbon Dioxide Removal (CDR) must complement conventional climate change mitigation efforts (Minx et al., 2018). One CDR technology under consideration is enhanced weathering (EW). EW relies on accelerating natural weathering reactions of silicate minerals with water (H_2O) and carbon dioxide (CO_2) (as in **Reactions 1 to 3**), which increases the concentration of base cations and dissolved inorganic C (DIC) in water, delivering inorganic CO_2 removal. In this study, we focus on DIC export from soils to the ocean, as this pathway is considered the most durable form of carbon sequestration (Phil Renforth & Henderson, 2017), rather than aiming to quantify a full greenhouse gas budget. DIC (the sum of aqueous [CO_2], [HCO_3^-] and [CO_3^{2-}]) can either be measured directly or estimated indirectly from total alkalinity (TA) or electrical conductivity, which are less expensive to monitor and can be empirically linked with DIC through calibration curves (Amann & Hartmann, 2022) (see also **Fig. S10**). This calibration is feasible because, according to the explicit conservative expression for TA in water, TA = [HCO_3^-] + [CO_3^{2-}] + [OH^-] – [H^+] (Wolf-Gladrow et al., 2007). TA can also be approximated from the sum of base cation charges, minus the sum of conservative anion charges (e.g. chloride, sulphate, phosphate, nitrate) (Barker, 2013; Wolf-Gladrow et al., 2007). DIC can also precipitate as soil inorganic carbon (SIC) in the form of solid carbonates, thereby losing half of the initially captured CO_2 (**Reaction 4**)(Haque et al., 2019). Inorganic CO_2 removal can be defined as the sum of changes in DIC leaching from a soil system after rock amendment plus the change in solid inorganic C (SIC) within the soil system after rock amendment. A robust and reliable accounting of Inorganic CO_2 removal must thus include both monitoring of DIC leaching and SIC changes.

$$Mg_2SiO_4 + 4CO_2 + 4\,H_2O \rightarrow 2\,Mg^{2+} + 4HCO_3^- + H_4SiO_4 \quad \textbf{Reaction 1}$$
(Mg-olivine weathering)

$$Ca_{0.5}Na_{0.5}Al_{1.5}Si_{2.5}O_8 + 1.5\,CO_2 + 8\,H_2O \rightarrow 0.5\,Na^+ + 0.5\,Ca^{2+} + 1.5\,HCO_3^- + 1.5\,Al(OH)_3 + 2.5\,H_4SiO_4 \quad \textbf{Reaction 2}$$
(plagioclase (labradorite) weathering)

$$MgCaSi_2O_6 + 4CO_2 + 6\,H_2O \rightarrow Ca^{2+} + Mg^{2+} + 4HCO_3^- + 2\,H_4SiO_4 \quad \textbf{Reaction 3}$$
(pyroxene (diopside) weathering)

$$2\,HCO_3^- + Ca^{2+} \rightarrow CaCO_3 + H2O + CO_2 \quad \textbf{Reaction 4}$$

EW is an attractive CDR technology for several reasons. First, EW may provide long-lived to permanent CO_2 sequestration: if fixed, DIC is transported via rivers or groundwater to oceans where it may not be released back into the atmosphere for millennia, the timescale needed for oceanic carbonate precipitation, which would release 50% of the DIC input back into the atmosphere (**Reaction 4**) (Renforth & Henderson, 2017). Secondly, rock dust amendment has the potential to improve soil fertility and counters soil acidification (Swoboda et al., 2021; Van Straaten, 2006). Thirdly, unlike some other CDR technologies (such as bio-energy with carbon capture and storage or afforestation), EW avoids competition for land with food production (Fuss et al., 2018; Janssens et al., 2022; Smith et al., 2016). Although several rock types are considered for EW, basalt is typically used in EW field trials and has several advantages. Basalt has relatively high base cation content, particularly of calcium (Ca) and magnesium (Mg), which translates into a high potential for CO_2 removal (Renforth et al., 2019). Additionally, basalt

is comprised of mafic silicate minerals such as plagioclases, pyroxene, and olivine, known for their relatively high weathering rates (Wr). Furthermore, basalt formations are abundant, widely distributed and close to major economies, making the adoption of EW using basalt scalable. Importantly, basalt is safer for agricultural application compared to ultramafic rocks like dunite due to its lower content of heavy metals such as nickel (Ni) and chromium (Cr) (Beerling et al., 2020).

Despite the great potential of terrestrial EW and substantial attention by industry in recent years, monitoring rock weathering and CDR is challenging. Quantification of Inorganic CO_2 removal by EW has often focussed on tracking DIC or alkalinity leaching in porewaters (Holzer et al., 2023; McDermott et al., 2024). However, it is also important to consider DIC in exported soil water (leachates)(Larkin et al., 2022) as changes in DIC during soil water transport are well-established. Numerous studies demonstrated that soil water movement and pH strongly govern DIC dynamics, both in soil research (Öquist et al., 2009; Schindlbacher et al., 2019) and in EW research (Dietzen et al., 2018; Niron et al., 2024; Reynaert et al., 2023; Vienne et al., 2024).

Focusing solely on changes in DIC and SIC may however overlook other critical soil processes that impact CDR. Besides the carbonate soil pool, other solid soil pools can also extract base cations from solution (**Figure 1**). These pools (temporarily) trap base cations, preventing DIC leaching and could stabilize soil organic matter (SOM) (Buss et al., 2024). Here, we trace the fate of cations in four different soil pools, to gain better estimates of Wrs and CDR.

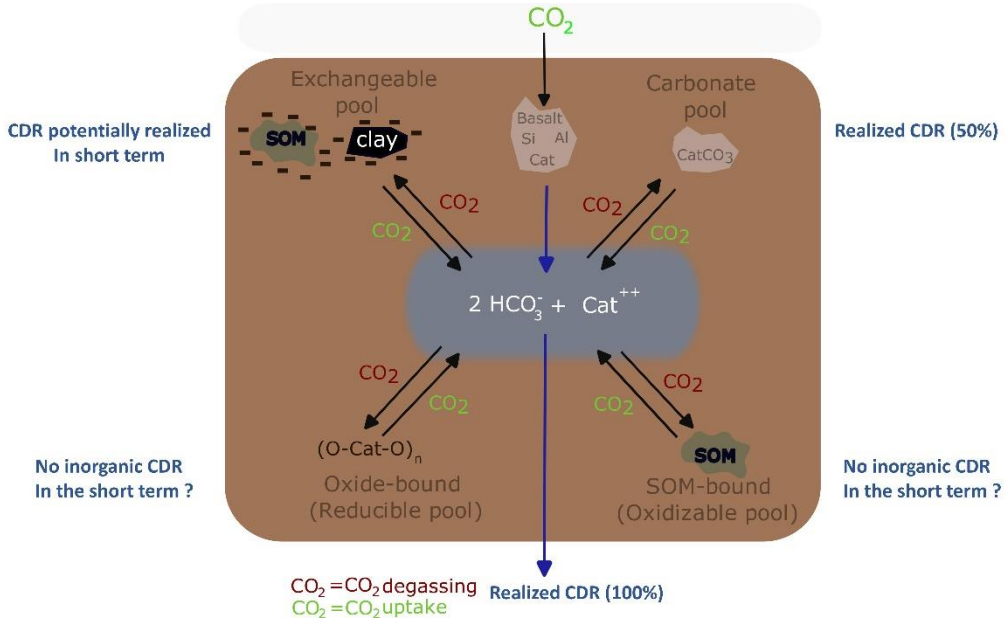

Figure 1: Schematized weathering of aluminosilicate rock and four soil pools that scavenge base cations (= alkalinity): exchangeable pool, carbonate pool, reducible pool and oxidizable pool. Because of charge balance, uptake of base cations by these pools releases H+ that can reconvert bicarbonate (HCO_3^-) (that was a priori generated from CO_2 through weathering) into CO_2. Cat++ = one divalent base cation or two monovalent base cations. In each corner, in blue, the significance for CDR is indicated for each of the soil pools.

Tracing base cations in soils can be done based on the established methodology of Tessier et al. (1979) in which cations are partitioned into four operationally defined soil pools; The exchangeable pool, the carbonate pool, the reducible pool and the oxidizable pool. First, in the exchangeable soil pool, cations interact with negatively charged clay or SOM surfaces. Secondly, the carbonate pool contains carbonates such as calcium carbonate ($CaCO_3$) and the C in this pool is reported as SIC. The detection of changes in SIC in basalt amended soils in short-duration experiments is typically challenging (Kelland et al., 2020; Vienne et al., 2022). Focusing on carbonate base cations may avoid typical issues with C heterogeneity and detection of relatively small SIC changes.

Thirdly, Tessier et al. (1979) operationally defined a reducible soil pool where base cations are associated with iron (Fe) and manganese (Mn) (hydr)oxides, and an oxidizable pool where cations are bound to SOM or sulfides. Dzombak & Morel (1990) modelled adsorption of Mg to hydrous ferric oxides (FeO(OH)), in which a surface hydroxyl group loses a proton and is replaced by a magnesium ion ($FeOOH + Mg2+ \Leftrightarrow FeOMg+ + H+$) and thereby decreases solute TA. In the fourth considered soil pool, the oxidizable pool, organic functional groups such as carboxylic and phenolic groups can form strong bounds with cations after deprotonation (Kalinichev et al., 2011). Cations in the oxidizable pool are expected to chemically stabilize organic matter due to cation bridging and inhibition of decomposing enzymes (Rowley et al., 2018).

In conclusion, base cations in these soil pools could decrease solute TA after proton release and hence degas DIC while potentially stabilizing SOM. Last, besides soil pools, also plants can scavenge base cations from solution. Base cations that go to the plant pool can be recycled to the aqueous phase, either through decomposition of plants in the field or through the food chain and sewage system, further complicating base cation mass balancing.

The undesirable side-effect of base cation scavenging (by plant/soil pools) is the release of protons to maintain charge balance. This release of protons converts negatively charged DIC (HCO_3^- and carbonate anions (CO_3^{2-})) to H_2CO_3, which is in equilibrium with gaseous CO_2 ($CO_3^{2-} + H^+ \rightarrow HCO_3^-$ and $HCO_3^- + H+ \rightarrow H_2CO_3 \Leftrightarrow H_2O + CO_2$ (g)). Hence, inorganic CO_2 removal can be reversed during temporary storage of base cations and realized again when base cations are released back from soil and plant pools into the aqueous phase.

From base cations in plant and soil pools, we can thus calculate a ‘potential inorganic CO_2 removal’, a terminology proposed by Steinwidder et al., (2025). This is a maximum quantity of Inorganic CO_2 removal that can be achieved when all cations released through silicate weathering are charge-balanced by bicarbonate/carbonates and leached from soils. Base cation retention in different soil pools results in a temporal decoupling between weathering and inorganic CO_2 removal. The timeframe in which the potential inorganic CO_2 removal can be achieved is a major uncertainty in EW (Kanzaki et al., 2025). For weakly bound exchangeable cations, potential inorganic CO_2 removal may be achieved in the relative short term of decades. Within this timeframe, because of stronger binding strengths, reducible and oxidizable base cations are more unlikely to be released and thus deliver inorganic CO_2 removal.

Last, inorganic CO_2 removal is only achieved if the weathering agent that induced the weathering was H_2CO_3 (as in Reaction 1-3). If the weathering agent is another acid (e.g. nitric acid (HNO_3) from fertilizers), no inorganic CO_2 removal occurs (McDermott et al., 2024; Taylor et al., 2021).

In a mesocosm experiment with basalt rock powder addition, we aimed to accurately quantify the Wr and potential inorganic CO_2 removal through quantification of base cations in the four abovementioned soil pools, soil water and maize plants. Tracing the fate of alkalinity after its generation by the weathering of primary minerals is key to accurately quantify basalt Wrs. Here, we make a mass balance after 101 days of experiment, investigate the fate of base cations through exploration of sequential extractions as a monitoring strategy for weathering and implications for C sequestration.

2. Materials and Methods

2.1 experimental set-up

A mesocosm experiment with 30 mesocosms was constructed at the experimental site at the Drie Eiken Campus of the University of Antwerp (Belgium). This experiment was part of a larger mesocosm experiment that aimed to investigate heavy metal fate and plant biomass in silicate amended maize plants (Rijnders et al., 2025). The mesocosms (0.6 m height, radius=0.25m) received natural rainfall and received additional water through manual irrigation (**Fig. S2**). In May 2021, the lower 40 cm of each mesocosm was filled with a slightly acidic sandy loam soil (**Table 1**).

Table 1: properties of control soil.

Control soil properties*	
pH (in a soil: water suspension (1:2.5))	5.66 ± 0.01
Texture (Sand, clay, silt %)	**Sandy loam** (61, 4, 35 %)
Soil organic C (SOC) (%)**	0.53 ± 0.01
SIC (%)	0.0031 ± 0.0002
Cation exchange capacity (CEC) (meq/100g)	3.03 ±0.11
Base saturation (%)	50 ± 5
Bulk density (BD) (kg/L)	1.58±0.02

*Reported values represent the average ± standard error (SE) of control soil sampled at all depths after the experimental period of 101 days. ** Determined through loss on ignition (4h heating at 360°C and assuming a SOC/SOM ratio of 0.58 (Van Bemmelen, 1890)).

The upper 20 cm was filled with the same soil, either unamended in the control treatment (5 mesocosms), or amended with basalt (**Figure 2**). Five mesocosms received 50 ton basalt ha^{-1}, while six others received different amounts of basalt, ranging between 10 and 200 ton ha^{-1} (**Table 2**). The basalt was mixed homogenously in the control soil using a concrete mixer. Basalt was obtained from DURABAS (https://www.rpbl.de). Particle size distribution (PSD) was analyzed using a mastersizer 2000 with a Hydro 2000G sample dispersion unit after removing larger particles with a 2 mm sieve. The P80 was 310.78 µm (see **Fig. S5**). The specific surface area (SSA) was determined with a Quantachrome Autosorb iQ using the Braunauer-Emmet-Teller (BET) method. The

measurement used nitrogen gas as adsorbate with multi-point (5 points) and isotherm (77K) settings. Samples with the same treatment were pooled in equal quantities into one sample to reduce the cost and time for analysis. All samples were degassed at 300 ^{o}C with 200 minutes of soak time. High measurement quality was ensured by frequent reference measurements (Bundesanstalt für Materialforschung und -prüfung, Germany) in addition to three technical repetitions for each measurement. The BET-SSA of the basalt rock was 9.226 ± 0. 08 m^2 g^{-1}. X-ray diffraction (XRD) and x-ray fluorescence (XRF) analyses are provided in the supplement.

Table 2: Overview of basalt application rates. The 0 and 50 t basalt ha-1 application rates were replicated in five mesocosms, while other application rates were only tested in one mesocosm. We added these replicates within individual application rates to learn about the variability between mesocosms receiving the same treatment.

Ton silicate ha^{-1} (replications)	0 (5x)	10	30	50 (5x)	75	100	150	200

Basalt was mixed into the top soil on 17/5/2021. To allow leachate collection, mesocosms had a 2 cm diameter hole at the bottom. On the inside, the bottom of the pot was covered with a root exclusion mesh to prevent soil export. Glass collectors (2.3L volume) were placed under the mesocosm to collect the leachates. Leachate volumes were determined throughout the experiment and were collected for chemical analyses on seven occasions. On 3/6/2021, two sweet maize seedlings (variety Tom Thumb) were planted in each the mesocosms and all pots received fertilization with nitrogen (N), phosphorus (P) and potassium (K) (96 – 10 – 79) kg ha^{-1} by adding Ca nitrate ($Ca(NO_3)_2$), triple super phosphate (TSP, 45% P_2O_5) and potassium sulfate (K_2SO_4). The experimental duration was 101 days; plants were harvested on 26/8/2021.

Soil water content and temperature were recorded using Cambell Scientific sensors (CS616) that are 30 cm in length. Watering (using rain water collected from a tank) was executed manually and total water manual inputs were tracked. In addition, daily precipitation amounts (in mm) were obtained for Wilrijk (Belgium) using the open source tool (visualcrossing.com). In the supplement, an overview of environmental conditions (rainfall, total water inputs, temperature and soil moisture) is given.

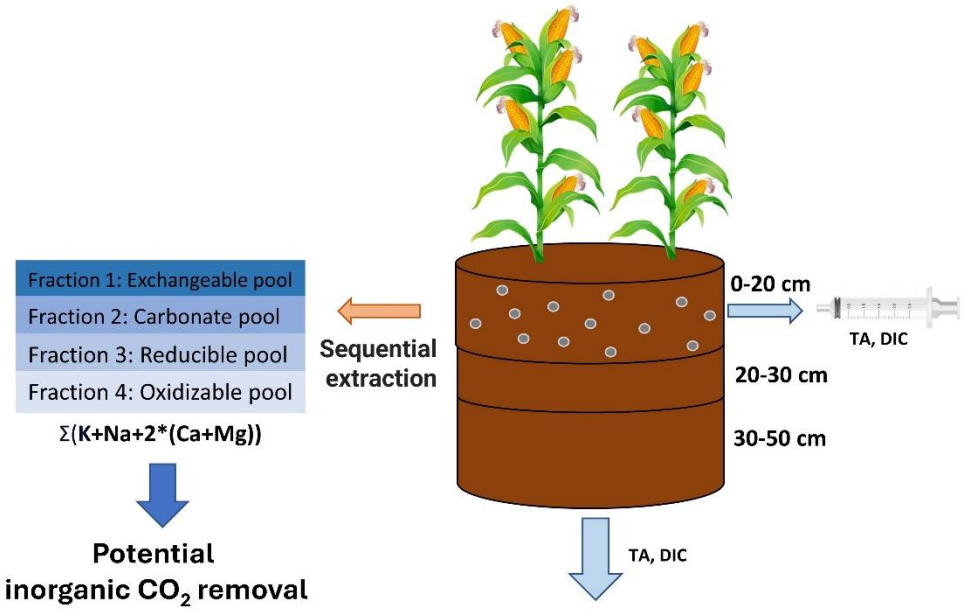

Figure 2: Overview of experimental set-up and measurements.

2.2 Leachate and pore water analysis

Weekly pore water sampling was performed with rhizons (Rhizon Flex, Rhizosphere Research Products B.V., Wageningen, NL) installed at 5 cm depth in each mesocosm. Leachate and porewater samples were filtered through a 0.45 µm PET filter. The major cations (Ca, Mg and K) were measured through ICP-OES (iCAP 6300 duo, Thermo Scientific). Before analysis, ICP samples were conserved using 1.5 mL (HNO_3 69%) per 30 mL sample. TA was determined using a SAN++ continuous flow analyzer (Skalar - NLD). The pH was measured using a HI3220 pH/ORP meter. Dissolved organic carbon (DOC) and DIC were measured using a FormacsHT with LAS sampler (Skalar - NLD). DIC and DOC were measured on eight and 12 occasions in leachates and pore water respectively.

Two quality control (QC) standards were analyzed for individual elements (Ca, K, Mg, sodium (Na), silicium (Si) and Fe). The mean precision of the QC standards was 0.84%, 1.12%, 0.54%, 2.79%, 1.67% and 1.30% for the respective elements. The mean accuracy for the two QC standards was 1.87%, 2.30%, 0.17%, 1.88%, 1.39% and 2.65% for Ca, K, Mg, Na, Si and Fe respectively. For TA soil water samples, mean accuracy and precision for two different QC standards were 1.51 and 1.72% respectively. The DIC measurements with FormacsHT had an accuracy and precision 1.09 and 0.23% respectively. Accuracy and precision were determined based on 12 measurements of a QC for TA (standards: 150 and 350 mg CaCO3 L^{-1}) and DIC (range between 10 and 100 mg L^{-1}) and based on eight measurements of two different QC concentrations for each individual element.

2.3 Soil collection and pretreatment

Top soil pH was measured on five dates. To determine top soil pH, 4 g of air dried topsoil sample was dissolved in 10 mL deionized water and shaken before pH measurement using a HI3220 pH/ORP meter (Hanna Instruments, Temse, Belgium). After harvesting, soils were sampled using cylindrical soil cores (100 cm^3, 5 cm length x 20 cm^2).

Samples were taken across the depth of the mesocosm and three sampling depths were considered (0-20cm, 20-30cm, 30-50cm). The cores were dried at 70°C for 48 hours to determine water content (gH_2O/g soil) and bulk density. An additional soil sample was taken at each depth, dried at 70 °C for 48 hours and used for chemical analyses.

2.4 Sequential base cation extractions

As conceptualized by Tessier et al. (1979), base cations can reside in four different soil pools: the exchangeable pool (where O-atoms on hydroxyl or carboxyl groups of clays or SOM associate with cations), the carbonate pool (cations bound in pedogenic carbonates), the reducible pool (cations bound to Al/Mn/Fe hydr(oxide)) and the oxidizable pool (cations bound to SOM). SOM bound to cations, extracted with weak salt solutions in the exchangeable pool typically has a low turnover time (Poeplau et al., 2018) and is therefore thought to be more susceptible to microbial decomposition than oxidizable SOM.

We adapted the original Tessier scheme by replacing 1M magnesium chloride with 1M ammonium acetate ($NH_4(CH_3COO)$) for extraction of the exchangeable pool, in order to be able to measure all base cations in the exchangeable pool. Likewise, Na-acetate was replaced with a mixture of acetic acid and water to be able to measure Na in the carbonate pool. We quantified SIC changes from the base cations in these acetic acid extracts (as in (Larkin et al., 2022)) (see also Equation S4). Additionally, three other SIC measurement techniques were explored to compare and the sensitivity of detecting SIC changes after amending with a range of basalt (see section S3.7).

Table 3: overview of sequential extraction method
(extraction time, temperature, conditions, volume of extractants and chemical composition of extractants).

Extraction scheme	**Extraction scheme** **Adapted** **Tessier et al. (1979)***
Pool 1: Exchangeable pool	10 mL 1M $NH_4(CH_3COO)$ 1h, 20°C, shaker → centrifuge → sample
Pool 2: Carbonate pool	5 mL 1M acetic acid (2h, 20°C, shaker) + 4 mL H2O + 1 mL 3M NH4Acetate → sample
Pool 3: Reducible pool	20mL 0.04M hydroxylamine ($NH_2OH.HCl$) in 25% (v/v) acetic acid (pH 2) 6h, 96°C, heat bath
Pool 4: Oxidizable pool	3mL 0.02M HNO_3 +5mL 30% peroxide (H_2O_2) (to pH 2 with HNO_3): 2h, 85°C, heat bath +3mL 30%H_2O_2 (to pH 2 with HNO_3) 3h, 85°C, heat bath +5mL 3.2M $NH_4(CH_3COO)$ (in 20 vol%HNO3) +4 mL H_2O 0.5h, 20°C, shaker

Prior to extractions, approximately 1g of soil was air dried. We also conducted the extractions for the pure basalt that was initially added to the mesocosms to be able to correct for the cations that were initially already present as exchangeable, carbonate, reducible and oxidizable pool cations. After each extraction, samples were centrifuged for 2 minutes at 2000 rpm, supernatants were collected for analysis. The remaining soil pellet after centrifugation was washed with 10 mL of demineralized water before the following step. Relevant elements (K, Na, Mg, Ca, Al, Fe and Si) were measured in each pool using ICP-OES (iCAP 6300 duo, Thermo Scientific) for each pool. Si was

only assessed in the reducible pool and in the oxidizable pool to investigate whether Si forms amorphous oxides or allophane-like compounds or binds with organic matter. Al carbonates were not quantified here as naturally these carbonates are not commonly formed (Takaya et al., 2019).

2.5 Plant responses

On 26/8/2021(101 days after basalt amendment in soils), the aboveground biomass was harvested and dried for 48h at 70 ºC to determine dry weight. Plant material was ground with an ultra-centrifugal mill (Model ZM 200, Retsch GmbH, Haan, Germany). Base cations (Ca, Mg and K) were measured through ICP-OES (iCAP 6300 duo, Thermo Scientific) in aboveground biomass to calculate plant base cation stocks. Base cations were measured separately in all aboveground biomass parts: stems, leaves, flowers and maize ears.

2.6 Calculation of Wr and potential inorganic CO_2 removal

We use the delta (∆) symbol to denote the difference relative to unamended control soil. Accordingly, we quantify ΔTA (the change in total alkalinity in the basalt-amended soil relative to the control) based on the difference in base cation concentrations between amended and unamended soils. As basalt only contains cations and no conservative anions, we assume that ∆TA can be quantified from the change in base cation charges (**Equation 1**).

$$\Delta\mathrm{TA} \approx 2 * (\Delta\mathrm{Ca} + \Delta\mathrm{Mg}) + \Delta\mathrm{Na} + \Delta\mathrm{K} - \Delta\text{conservative anions} \quad with\ \Delta\text{conservative anions} = 0 \qquad (\mathbf{1})$$

The Wr corresponds to the rate of rock dissolution. The Wr can be expressed per element or as moles of alkalinity equivalents (i.e. the sum of base cation charges (**Equation 1**) per amount of rock surface area per unit of time (in mol m^{-2} rock s^{-1}). In addition, we calculate a 'potential inorganic CO_2 removal'. We use the same definition for potential inorganic CO_2 removal as in Steinwidder et al. (2025). A 'potential inorganic CO_2 removal' can be defined as the maximum amount of inorganic CO_2 that could be removed if all experimentally determined, weathered, soil-retained base cations were to leach from the soil and be completely balanced by carbonate anions. Potential inorganic CO_2 removal was previously 'CDR potential' by Niron et al. (2024)). The concept of CDR potential was first introduced by Phil Renforth (2019) to describe the maximum inorganic CO_2 removal achievable if all base cations within a rock were to completely weather. More recently, Beerling et al., (2024) quantified base cation losses from topsoils using an immobile/mobile tracer approach (see Section 4.2), from which they also derived a measure of CDR potential. To maintain conceptual clarity, we avoid using the term CDR potential for purposes other than its original definition by Renforth (2019). When the term is employed, its meaning should always be explicitly stated.

To calculate the Wr (from all base cation increases relative to controls in plants, extracted soil fractions and soil water leachates), we sum changes in TA in the following pools: exported soil water (leachates), plants and soil pools.We can express changes in the cation pool of each reservoir as the equivalent Wr required to supply the

cations ($Wr_{leachate}$, Wr_{plant} and Wr_{soil}) (**Equation 2**). Conventionally Wrs are expressed using a logarithmic scale as absolute values can vary strongly.

$$Log\ Wr\left[\frac{\Delta mol\ TA}{m^2 rock.s}\right] = Log\left(\frac{\Delta mol\ TA_{soil} + \Delta mol\ TA_{plant} + \Delta mol\ TA_{leachate}}{m^2 rock.s}\right) \quad (2)$$

We used a gradient of rock applications, where we calculated the slope of the molar change in base cation charges (expressed as an equivalent "alkalinity" change if these base cations were dissolved in water) with higher rock amendment (TA slope) (**Figure 3)**. We compared logarithmic and linear regression and selected the linear regression approach, as both approaches had comparable R^2 and Akaike Information Criterion (AIC) values values and linear slopes ease further data processing (**Fig. S23 and Table S5**). We opted for the linear regression approach to simplify subsequent calculations. To make our gradient approach more robust, we also calculated the log Wr for individual application rates in **Fig. S13.**

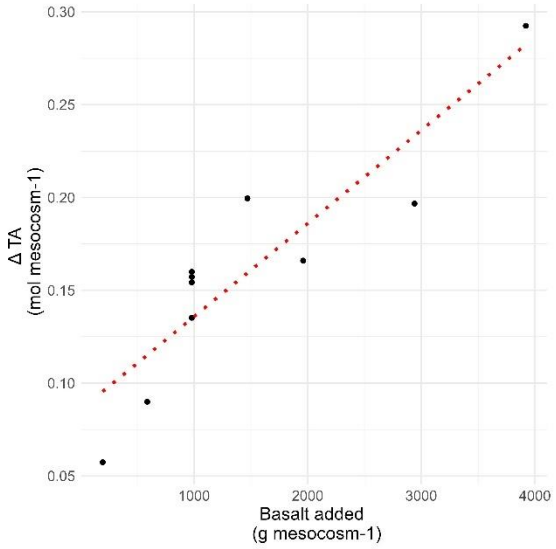

Figure 3: Illustration of the calculation of TA slope: The alkalinity scavenging by a given pool was plotted in function of the applied basalt, after which the slope was used to quantify a Wr. This figure is an example regression with data for the top soil exchangeable pool. All regressions can be found in **Fig. S22.**

Then we converted units of the alkalinity slope for increasing rock application (TA slope) per unit of rock mass to moles of alkalinity per rock surface area and per time (**Equation 3**). Equation 3 was used to calculate Δmol TA m^{-2} rock s^{-1} of base cations in leachates, plants and of every measured soil pool at every soil depth.

$$\frac{\Delta mol\ TA}{m^2\ rock.s} = \frac{\textbf{Scavenged alkalinity } (= \textbf{TA slope}) \left[\frac{\Delta mol\ TA}{g\ rock}\right]}{Experimental\ duration\ [s] * SSA_{silicate} \left[\frac{m^2 surface\ area}{g\ rock}\right]} \quad (3)$$

Δmol TA m^{-2} rock s^{-1} was thus quantified per pool, based on the change in base cations in the basalt treatment compared to the control treatment. For plants, we calculate TA slope through regression of harvested base cations

with basalt application. Harvested base cations were calculated as the product of harvested aboveground biomass and their base cation content. Charge contributions of Na were not included; Na was not quantified at the time of plant biomass elemental analysis, which may lead to an underestimation of the alkalinity equivalent increase in the plant pool. However, given that base cation charges in the plant pool were about two orders of magnitude smaller than in the soil pool, we expect the effect of this omission to be limited. In addition, maize plants aim to actively increase their K/Na ratio which avoids salt stress, the K content of maize shoots is typically about 2 orders of magnitude larger than Na (Gao et al., 2016; Suarez & Grieve, 1988). For leachates, TA slope was calculated as the product of mean cumulative leachate volume and mean leachate TA concentration for each application rate and regressing them with the applied basalt as dependent variable.

Finally, the Wr attributable to the change in cation content of the soil pools ($Wr_{soil.}$) was calculated by summing the $Wr_{soil\_layer\_k\_pool\_j}$ for each pool and depth (**Equation 4**). Here, we sum changes in all pools of the topsoil (0-20 cm) and lower depths (20-30 cm and 30-50 cm) to obtain an aggregate value for $Wr_{soil.}$ With $\boldsymbol{Wr_{soil,layer\,k,\ \ fraction\,j}}$ calculated as in **Equation 4** (with k = the number of depths and j = the number of considered soil pools). TA slope at every depth and soil pool was calculated as in **Equation 5.**

$$\boldsymbol{Wr_{soil}} = \sum_{k=1}^{3} \sum_{j=1}^{4} \boldsymbol{Wr_{soil,layer\,k,\ \ pool\,j}} \qquad (\mathbf{4})$$

$$\boldsymbol{scavenged\ TA}\ (\text{TA slope})\left[\frac{\boldsymbol{\Delta mol}}{\boldsymbol{g\ rock}}\right] = \frac{\frac{\mu \boldsymbol{mol\ TA}}{\boldsymbol{g\ dry\ Soil}}(\boldsymbol{Amended\ Soil}) - \frac{\mu \boldsymbol{mol\ TA}}{\boldsymbol{g\ dry\ Soil}}(\boldsymbol{control\ Soil})}{\boldsymbol{Application\ rate\ (Amended\ soil)}\ [\boldsymbol{g\ rock\ m^{-2}\ ground\ area}] * \mathbf{1000}} * \boldsymbol{Bulk\ Density}\left[\frac{\boldsymbol{kg\ dry\ Soil}}{\boldsymbol{m^3 soil}}\right] * \boldsymbol{thickness\ soil\ layer}\ [\boldsymbol{m}] \qquad (\mathbf{5})$$

Equivalents of soil retained base cation charge equivalents per gram of dry soil mixture can be calculated for each mesocosm by summing the charges from each base cation (**Equation 6)**.

$$\frac{\mu \boldsymbol{mol\ TA}}{\boldsymbol{g\ dry\ Soil}} = \sum_{j=1}^{4} \left(\frac{\frac{\mu \boldsymbol{g\ Ca_{pool_j}}}{\boldsymbol{g\ dry\ soil}}}{\mathbf{40.078}\frac{\boldsymbol{gCa}}{\boldsymbol{molCa}}} + \frac{\frac{\mu \boldsymbol{g\ Mg_{pool_j}}}{\boldsymbol{g\ dry\ soil}}}{\mathbf{24.305}\frac{\boldsymbol{gMg}}{\boldsymbol{molMg}}} \right) * \frac{\boldsymbol{2mol\ TA}}{\boldsymbol{mol\ cat^{++}}} + \left(\frac{\frac{\mu \boldsymbol{g\ Na_{pool_j}}}{\boldsymbol{g\ dry\ soil}}}{\mathbf{22.990}\frac{\boldsymbol{gNa}}{\boldsymbol{molNa}}} + \frac{\frac{\mu \boldsymbol{g\ K_{pool_j}}}{\boldsymbol{g\ dry\ soil}}}{\mathbf{39.098}\frac{\boldsymbol{gK}}{\boldsymbol{molK}}} \right) * \frac{\boldsymbol{1molTA}}{\boldsymbol{mol\ cat^{+}}} \qquad (\mathbf{6})$$

These individual base cations (e.g. Ca in pool j) are calculated from the difference of cations weathered during the weathering operation minus the cations initially present in that fraction in the applied feedstock (Power et al., 2025) (**Equation 7**). For example, some cations can already exchange on the surface or edges of the applied minerals, so that these cannot be counted as weathered, they will however contribute to CDR once leached.

To calculate in-situ Wr, it is thus necessary to correct for the cations that had already been weathered from primary minerals at the time of silicate amendment. This correction is currently not being done in EW literature yet. As basalt is only added to the top soil and not deeper, this correction is only done for the 0-20 cm soil layer here.

$$\frac{\mu g\ element_{i_{pool\ j}}}{g\ dry\ soil} = \left(\frac{\mu g\ element_{i_{pool\ j}}}{g\ dry\ soil}\right)_{Post\ weathering,\ soil\ mixture} - \left(\frac{\mu g\ element_{i_{pool\ j}}}{g\ dry\ soil}\right)_{added\ with\ feedstock\ initially} \quad (7)$$

The mass of a specific element (i) in each of the four (j) soil pools (in µg element/g soil) is calculated using **Equation 8.**

$$\left(\frac{\mu g\ element_{i_{pool\ j}}}{g\ dry\ soil}\right)_{Post\ weathering,\ soil\ mixture} = \frac{concentration\ element_i\ in\ pool_j\ \left[\frac{mg}{L}\right] * Volume\ extract_j[mL]}{mass\ of\ solid\ extracted\ [g]} \quad (8)$$

The initial addition of element i to pool j is calculated as in **Equation 9**.

$$\left(\frac{\mu g\ element_{i_{pool\ j}}}{g\ dry\ soil}\right)_{added\ with\ feedstock\ initially} = \frac{\mu g\ element_i\ pool_j}{g\ silicate} * \frac{Application\ rate\ \left[\frac{g\ silicate}{m^2}\right]}{Bulk\ density\ \left[g\ dry\frac{soil}{m^3}\right] * depth\ of\ soil\ amendment\ [m]} \quad (9)$$

According to the charge balance (**Reaction 1-3)** during mineral dissolution, 1 mol HCO_3^- mol^{-1} TA is generated (and thus 1 mol of CO_2 is sequestered). We define a factor η, that is equal to the ratio of HCO_3^- per mol of generated TA. According to charge balance, η=1. A more conservative approach is to assume that all this generated alkalinity will be exported to the ocean, after which chemical equilibrium degasses a portion of the alkalinity (η = 0.7 mol CO_2 mol^{-1} TA, assumed for oceans) (Renforth et al., 2012; Renforth et al., 2019; Renforth & Henderson, 2017). According to Renforth et al. (2019), the ocean alkalinization efficiency η ranged between 0.7 and 0.85. This η parameter is relatively uncertain given that model studies indicate that η can range between 0.65 and 0.8 mol CO2 mol TA^{-1} (see section S6 in the supplement of (Kowalczyk et al., 2024)). Alternatively, we can assume that all base cations will form solid carbonates in soils or rivers. In this case η=0.5 mol CO_2 mol^{-1} TA (**Reaction 4**). In **Table 4**, we calculated potential inorganic CO2 removals assuming conservative values of η=0.5 (carbonate precipitation scenario) and η=1 (the highest possible η without any downstream DIC losses).

While calculating Wr, cations added with the rock feedstock that were already weathered were subtracted as in **Equation 7**, yet these cations are not subtracted to calculate the potential inorganic CO_2 removal as base cations in weathered fractions of the rock feedstock can also leach to soil water whereby HCO_3^- is generated. Last, base cation changes in the plant pool were excluded from the potential inorganic CO_2 removal pool here, as a conservative approach we assume that base cations in plants will not reach the ocean. The latter assumption had a negligible impact on the potential inorganic CO_2 removal estimate (**Table 4**).

$$potential\ inorganic\ CO_2\ removal\ \left[\frac{kg\ CO2}{t\ rock}\right] = Scavenged\ TA\ \left[\frac{mol\ TA}{g\ rock}\right] * \frac{\eta\ molCO2}{mol\ TA} * \frac{44gCO2}{mol\ CO2} * 1000 \quad (10)$$
$$with\left(\frac{\mu g\ element_{i_{pool\ j}}}{g\ dry\ soil}\right)_{added\ with\ feedstock\ initially} = 0$$

2.7 Calculation of the carbonate saturation indices (SIc) using Phreeqc

To assess whether carbonate precipitation was theoretically possible during this experiment, we calculated SIc for dolomite and calcite. For Mg and Ca the SIc as the logarithm of the ion activity product and the solubility product constant if dolomite and calcite (SIc = log IAP/K). Minerals have the potential to precipitate when a log SIc >0 is

reached although substantial oversaturation of calcite (log SIc > 1) without calcite formation is possible in rivers due to ion inhibition, e.g. by phosphate (Morse et al., 2007; Zhang et al., 2022). Likewise, they are in equilibrium at a log SIc =0 and dissolve if log SIc <0. The R phreeqc package was used and the phreeqc.dat database was used. As an input, the experimental pore water (10 cm depth) composition of Mg and Ca was entered, as well as measured pH and TA. Daily SIc values were calculated by feeding unique combinations of Mg, Ca, pH and into the PHREEQC solution function for each day.

2.8 Data analysis

For SIC and elemental stocks in plant biomass, soil pools and soil water export, a linear regression with basalt application rate as a dependent variable was performed to test for a basalt effect. For measurements that were repeated in time (pore water and leachate DIC and DOC compositions), a linear mixed model was used with basalt and time as fixed factors and mesocosm as a random factor using the lme4 R package (version 1.1-33). For measurements repeated in time, we assessed basalt x time interaction effects and discarded these if not significant. All analyses were executed in R version 4.3.2. As an additional sensitivity analysis for the determination of Wr using the slope of application rates approach described in the main text, we quantified Wr also for individual application rates in **Fig. S13**.

To propagate uncertainty between basalt and controls in Figure 5, averages and standard errors for every replicated application rate (0 or 50 t/ha) were determined. The average from the 50 t ha-1 was subtracted with the average from the control soil and se = √ (se_control^2 + se_basalt^2). For non-replicated application rates (10,30, 75,100, 150 and 200 t/ha, se=0) the measurement was subtracted from the control soil average and errors were also propagated with se = √ (se_control^2 + se_basalt^2).

3 Results

Basalt amendment significantly increased DIC and TA in the top soil water (**Figure 4**). TA in soil water correlated positively with DIC (R^2 = 0.68, p<0.01, **Fig. S10**). TA was thus generated in the basalt amended soil layer, yet we did not observe DIC or TA increases with higher basalt application rates in water exported from the soil column at 60 cm depth (**Figure 4**). Temporal dynamics show that DIC in top soil pore water gradually increased in time with higher basalt amendment, while DOC decreased in time with more basalt (**Fig. S7 and Table S4)**.

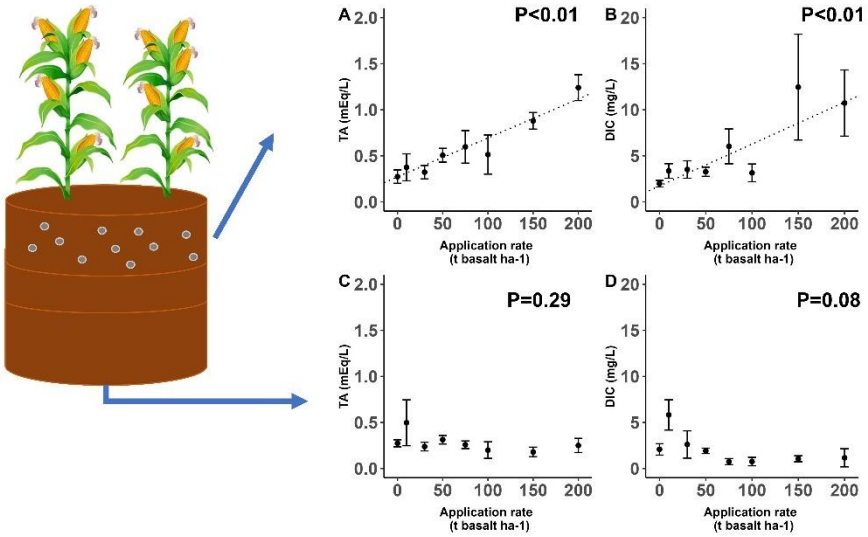

Figure 4: Top soil (0-20 cm) pore water (A) TA and (B) DIC concentrations. Export water (50 cm depth) (C) TA and (D) DIC concentrations. Values represent average concentrations +- standard error across all sampling occasions over the 101 day duration experiment (n= 125, 44, 95 and 60 for pore water DIC, TA and leachate DIC and TA concentrations respectively). Significant trends are indicated with a dotted regression line. Raw data for TA and DIC in function of time is visualized in **Fig. S7(B,D)** and **Fig. S9(B,D)**.

Overall, base cations were mostly retained in the top soil, where Ca significantly increased in the exchangeable, reducible and oxidizable pools with higher basalt addition. Only in the carbonate soil pool, Ca (and also Mg) significantly decreased with more basalt (**Figure 5 and 6**). With higher rock amendment, Mg accumulated in the top soil exchangeable pool ($p<0.01$). The Mg accumulation in the reducible pool was higher compared to the exchangeable, but the slope was borderline significant for the reducible pool ($p=0.07$) due to higher variability in Mg concentrations with increasing basalt amendment.

Changes in Na followed similar patterns as Mg, as also significantly more Na exchanged in top soil ($p=0.02$) and a larger signal of reducible Na was found ($p<0.01$). In contrast with divalent cations, monovalent cations increased in the carbonate fraction if basalt increased (**Figure 5 and 6**). With more basalt, Al is being found in association with the oxidizable and reducible fraction. Si increased only significantly in the oxidizable pool ($p=0.04$) (**Fig. S15**). Increases in oxidizable Si, Ca, Al with higher basalt addition suggest the formation of mineral-associated organic matter.

In the soil layer just below the soil-basalt mixture (20-30 cm), the cations did not increase significantly in any of the measured soil pools and oxidizable Na, Fe and Mg decreased significantly (**Fig. S11, Figure 6)**. We did not observe significant changes in any element with higher basalt amendment in the 30-50 cm soil layer (**Fig. S12).**

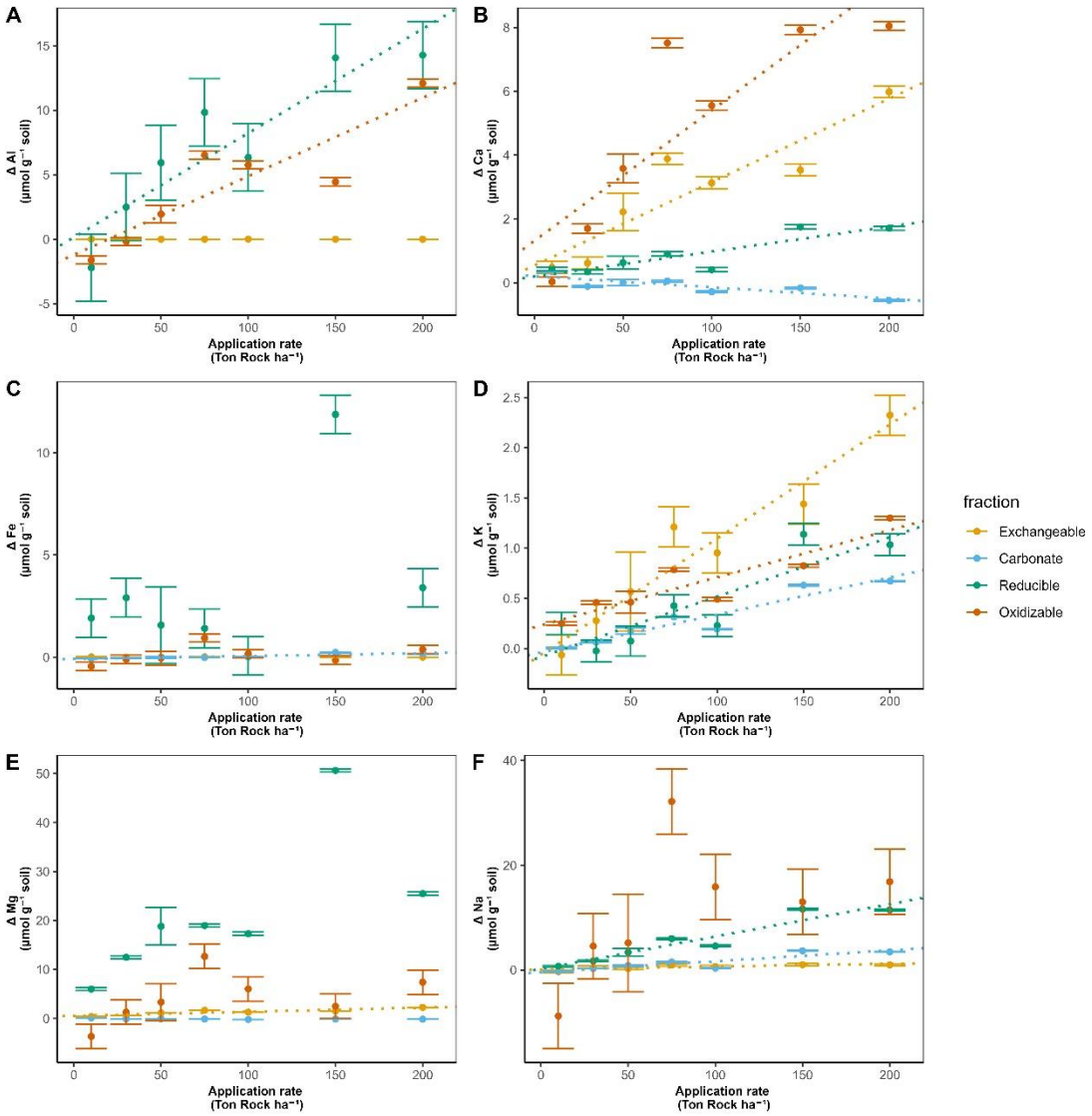

Figure 5: Change in top soil (0-20 cm) elements relative to the control soil (corrected as in **Equation 7**), 101 days after basalt amendment, as a function of basalt application rate for (A) Al (B) Ca (C) Fe (D) K (E) Mg and (F) Na for four different soil pools. Dots and error bars represent averages and standard errors. For basalt application rates other than 50 t ha^{-1}, error bars correspond to those of the control soils, as these basalt treatments were not replicated and the data are shown as control-normalized results. Significant effects ($p<0.05$) of basalt application rate on cation concentrations are indicated by dotted linear regression lines. Measurements were repeated on at least four samples per fraction for the control soils (N ≥4 for each fraction) and N=4 for 50 t ha^{-1} treatment (fewer than 5 replicates were available due to technical issues). Note that y-axes scales differ among subplots to better visualize small changes for some elements. Unnormalized (raw) data are presented in **Fig. S19-21.**

From all significant element changes in soil pools, we calculate that 8.4%, 52.1% and 9.4% Of basalt Na, K and Ca were weathered while we do not observe an increase in Mg if we only consider significant ($p<0.05$) slopes. If we consider all (also $p>0.05$) regression slopes, the estimates become 48.0%, 10.6%, 9.35% for K, Ca and Mg, while Na did not increase in this approach (mass balance per element, see **Fig. S23).**

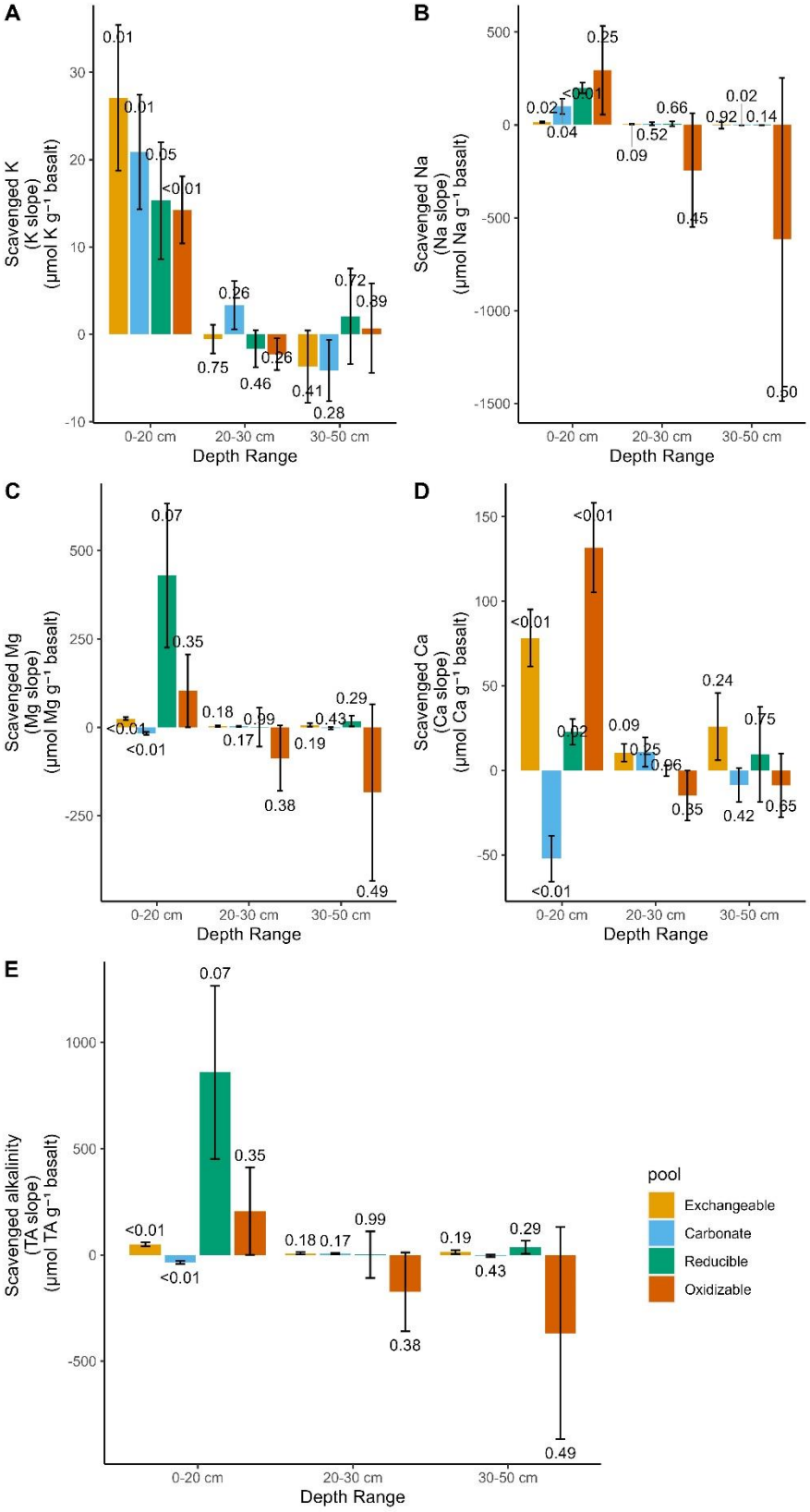

Figure 6: Equivalent alkalinity uptake 101 days after basalt amendment in different soil pools and depths. P-values of linear regressions are shown above and below bar plots of positive and negative changes respectively. Error bars represent the standard error that was derived from linear regression. Underlying regressions for slopes of TA scavenged by each pool and depth can be found in **Fig. S22**. Base cation changes in top soil pore water are not included in this figure as we only include charge equivalent adsorbed by soil pools here, yet base cations in top soil pore water were negligible (see **Fig. S24**).

Base cations were not only scavenged by soils, but also by plants. Although two orders of magnitude smaller than in soil pools, TA scavenging by plants was higher than soil water exported TA and increased significantly with larger basalt amendment ($p<0.01$) (**Figure 7**). The increase in base cation charges in plants was attributed to K (81%), Ca (11%) and Mg (8%).

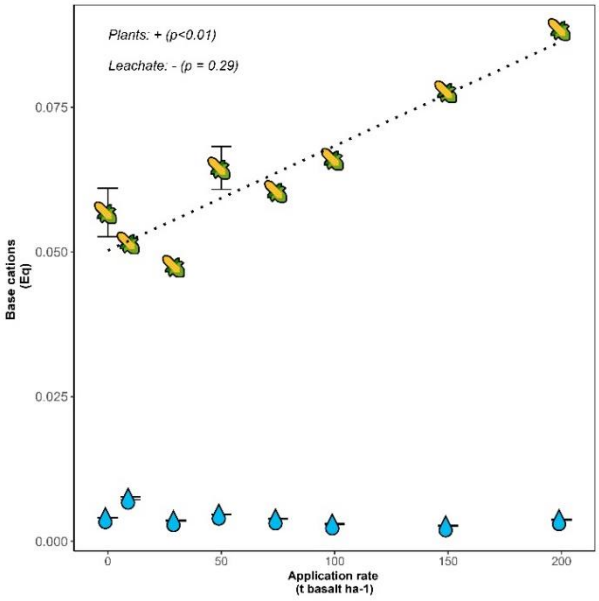

. **Figure 7:** Moles of base cation charge equivalent (Eq) per mesocosm after 101 days retained in maize plants (stems, leaves and maize ears), indicated with maize fruit symbols, and flushed with leaching water, indicated with droplets. Error bars represent averages and standard errors (n=5 for both control and 50 t ha^{-1} basalt replicates for plant measurements). For leachate TA, a total of 60 measurements were done in total at different dates. Na was not analyzed in plants and is thus not included in the harvested base cations. Errors on leachate TA were small and appear as horizontal lines within the droplets. Raw data for leachate TA measurements can be found in **Fig S9D.**

Converting the base cations to moles of equivalent TA and considering only the exchangeable pool as only soil cation reservoir we derive a log weathering rate of -12.13± 0.34 mol TA m^{-2} rock s^{-1} (**Table 4**). When we consider also the decrease in base cation equivalents in the carbonate pool, the mean estimate decreases to -12.23 mol TA m^{-2} rock s^{-1} , translating into mean estimated potential inorganic CO_2 removals of 0.36-0.5 kg CO_2 t^{-1} basalt (assuming η=0.5-0.7). If we include all soil pools and non significant regressions the estimates becomes one order of magnitude higher, yet with substantial uncertainty.

Table 4: Overview of the Wr and potential inorganic CO_2 removal that can be quantified from changes in base cations in specific soil pools. Rows where (scavenged) TA increased significantly with increasing basalt amendment are indicated in bold.

Soil Pool	Depth	Reservoir	Log Wr (Log mol TA/m² basalt /s)	CDR Potential* (kg CO2/ton basalt) (η = 0.5)	CDR Potential* (kg CO2/ton basalt) (η = 1)
/	/	Plant*	**-12.93±0.07**	**/**	**/**
/	/	Leachate*	**Wr<0**	**/**	**/**
Exchangeable	0-20cm	soil	**-12.20±0.41**	**1.10±0.04**	**2.21±0.07**
Carbonate	0-20cm	soil	**Wr<0**	**-0.75±0.03**	**-1.50±0.06**
Reducible	0-20cm	soil	-10.96±0.21	18.91±1.76	37.82±3.51
Oxidizable	0-20cm	soil	-11.58±0.43	4.53±0.89	9.06±1.77
Exchangeable	20-30cm	soil	-13.02±0.29	0.17±0.02	0.34±0.04
Carbonate	20-30cm	soil	-13.17±0.29	0.12±0.02	0.23±0.03
Reducible	20-30cm	soil	-13.17±50.43	0.02±0.47	0.04±0.95
Oxidizable	20-30cm	soil	Wr<0	-3.82±0.80	-7.56±1.60
Exchangeable	30-50cm	soil	-12.76±0.30	0.30±0.04	0.61±0.08
Carbonate	30-50cm	soil	Wr<0	-0.10±0.02	-0.21±0.05
Reducible	30-50cm	soil	-12.34±1.15	0.79±0.13	1.58±0.27

Oxidizable	30-50cm	soil	Wr<0	-8.10±2.15	-16.19±4.31
Exchangeable	0-20	Exchangeable+plant+leachate	**-12.13±0.34**	**1.30±0.04**	**2.21±0.07**
Exchangeable + Carbonate	0-20	Exchangeable+plant+leachate+ carbonate	**-12.23±1.05**	**0.36±0.05**	**0.71±0.10**
All soil pools	All	All soil pools + plant + leachate	-11.11±2.70**	13.17±3.07	26.33±6.13

*For leachates (which represents realized CDR) and also for plants there is no potential inorganic CO_2 removal in this approach. ** Abs (Wr/standard error (Wr)*LN(10)) was used to propagate the error using the log10 transformation, resulting in substantial uncertainty for the Wr estimate of all pools.

4. Discussion

4.1 Weathering rates and CO_2 removal

EW is typically considered as a durable CDR pathway that removes CO_2 from the atmosphere by producing DIC that is either transported to the ocean (Strefler et al., 2018) or precipitates as carbonates in the soil (Manning et al., 2013). Here, we observe a clear weathering signal (a TA and DIC increase) in top soil pore water (**Figure 4**). These TA and DIC increases in the pore water of amended top soil are consistent with recent findings (Holzer et al., 2023; McDermott et al., 2024; Vienne et al., 2024). Increased DIC in basalt soils relative to controls may result from enhanced plant root respiration or DIC exudation or from mineral weathering; our dataset does not allow these effects to be separated. DIC did however not leach from our soil columns within this experimental timeframe of 101 days.

Absence of substantial DIC leaching is in line with other short-term recent studies (Amann et al., 2020; Larkin et al., 2022; Niron et al., 2024; Vienne et al., 2024). For example, the log Wr of approximately -13 mol TA m^2 s^{-1} quantified from DIC export after 1 year in a mesocosm trial with 220 ton ha^{-1} olivine-rich rock (Amann et al., 2020) was about three orders of magnitude lower than what would be expected from lab-scale weathering studies (roughly -10 mol TA m^2 s^{-1}, (Palandri & Kharaka, 2004)). Vienne et al. (2024), amended soils with 100 ton basalt ha^{-1} and quantified a CDR from exported TA that was in the same order of magnitude as in the work of Amann et al. (2020). Although the studies of Amann et al. (2020), Vienne et al. (2024) were relatively short (<= 1 year) and used a relatively low water infiltration flux, also a longer (3 year duration) catchment-scale study in Malaysian oil palm plantations with high annual rainfall (>2000 mm $year^{-1}$) detected no significant increase in TA leaching in the catchments (Larkin et al., 2022). There may thus be a substantial delay for DIC leaching.

A DIC leaching delay can have multiple causes (**Figure 1**); A first possibility is pedogenic carbonate formation. We observe that solid carbonates did not increase in our experiment, in contrast, SIC decreased in time. PHREEQC calculations for our experiment suggest that dolomite and calcite were undersaturated, so that carbonate dissolution was possible (**Fig. S17)**. Saturation states are expected to be low in our experiment because control soil was undersaturated and dissolved base cations accumulated in other soil pools than the carbonate pool (**Figure 5 and 6**). A decrease in SIC is in contrast with substantial SIC increases found after wollastonite rock amendment (Haque

et al., 2019, 2020). The observed SIC increase in the latter field study may be partly attributed to residual carbonates from prior liming activities instead of new carbonate formation related to silicate weathering (Haque et al., 2020). Thus, not all measured SIC may reflect new carbonate formation in the study of Haque et al. (2020). For short-term basalt studies, using elemental C analysis, also no significant changes in SIC could be detected previously (Kelland et al., 2020; Vienne et al., 2022, 2024). In contrast, in the study of Larkin et al. (2022), a relatively small SIC increase was detected in amended soils, using carbonate pool extractions.

While TA was not exported or taken up by soil carbonates here and plant base cation losses were minor (**Table 4**) it was retained in top soil where the exchangeable and reducible pools reduced solute TA. We expect cations to be primarily associated with Fe- and Mn-(oxyhydr)oxides in the reducible pool and with organic matter in the oxidizable pool, as supported by literature (Tessier et al., 1979); However, the extraction chemicals of this sequential extraction scheme (hydroxylamine and H_2O_2) are known to have a limited specificity and may have also partially targeted other mineral phases (such as clays) (Ryan et al., 2008), which could explain the elevated Si observed in the topsoil pools (**Fig. S15**). In addition, the observed increase of aluminum in association with the reducible soil fraction indicate the formation of secondary minerals. While we cannot pinpoint the exact Mg-phases formed in our soils, our results do demonstrate substantial base cation retention in the soil and show that there can be more base cation losses to soils than to the exchangeable pool alone.

Our estimate of log Wr, derived solely from significant increases in TA uptake at higher basalt amendment rates, was approximately –12 mol TA m^{-2} s^{-1}. This estimate reflects changes in the exchangeable and carbonate soil pools, plant uptake, and leachate composition. Notably, this value aligns with previous studies that estimated log Wr values between –12 and –11 based on base cation depletion from the exchangeable pool alone (Kelland et al., 2020; Reershemius et al., 2023; te Pas et al., 2023), as summarized in Vienne et al., (2024). Also in a batch leaching experiment with 1mM $CaCl_2$ (designed to mimic soil solutions) the quantified log Wr of basalt was found to be -11 (Van Der Bauwhede et al., 2024).

Estimates from Buckingham et al. (2022), based only on leachates, gave a much lower log Wr of -15, partly due to low water infiltration rates. With a high infiltration flux (8000 mm/year), Amann et al. (2022) estimated log Wr between -12.5 and -13.5 from basalt leachates. This highlights the importance of including scavenged alkalinity to determine Wr in soils. When we also include non-significant regression slopes we derive a mean log Wr estimate with substantial uncertainty (-11.11±2.70) mol TA m^{-2} s^{-1}. From individual application rates, we quantify log Wr ranging between -11 and -10 (**Fig. S13**); These values are comparable to those observed in soil-free, laboratory-scale basalt dissolution experiments conducted at circumneutral pH (Brantley et al., 2008; Gislason & Oelkers, 2003). They also approximate the dissolution rates of key mineralogical components in basalt (such as plagioclases

(between -12 and -9 for Na and Ca endmembers respectively) and augite (-11.97)) under room temperature and neutral pH conditions (Gudbrandsson et al., 2011; Hermanska et al., 2022; Palandri & Kharaka, 2004a).

Although this and other experiments show relatively consistent weathering rates from exchangeable base cations (comparable to those observed in lab-scale studies) we emphasize that, unlike laboratory conditions where base cations remain far from equilibrium in excess water, soils experience solid-phase cation scavenging, which promotes DIC degassing (**Figure 1**). From the sum of significant TA slopes we calculate a relatively low potential inorganic CO_2 removal, equalling to approximately 0.36-0.71 kg CO_2 ton^{-1} basalt or 0.018-0.036 tCO_2 ha^{-1} for a basalt application rate of 50 t ha^{-1} (**Table 4**). Also the highest possible potential inorganic CO_2 removal realized within this experimental timeframe is modest; Including also non-significant TA increases and assuming $\eta = 1$, the potential inorganic CO_2 removal is quantified to be 26.33±6.13 kg CO_2 ton^{-1} basalt (**Table 4**). We emphasize that a potential inorganic CO_2 removal is a maximum inorganic CO_2 removal that can be realized with the delivered amount of base cation weathering as strong acids associated with fertilizers (such as nitric acid and sulphuric acid), or organic acids and not carbonic acid may have initially weathered silicate rock which does not lead to a CDR within the soil system (McDermott et al., 2024; Taylor et al., 2021). Moreover, life-cycle emissions associated with mining, grinding and transporting rock are typically of the same order of magnitude as our relatively low potential inorganic CO_2 removal (Lefebvre et al., 2019).

Furthermore, for climate change mitigation, not only the amount of potential inorganic CO_2 removal is important, but also the timescale at which this CDR is realized (Kanzaki et al., 2025). A mass balance of base cations indicates that exported TA was negligible compared to base cation charges that were retained in the soil over the timeframe of our experiment (101 days) (**Table 4**). As long as TA is retained in soil pools, inorganic CO_2 removal through DIC export is delayed as equivalent amounts of protons have then been released into the soil water to maintain charge balance (**Figure 1**). Realization of this delayed inorganic CO_2 removal depends on liberation of base cations from these soil pools and their transport out of the soil, charge-balanced by HCO_3^-. This export may take decades or longer, depending on the circumstances (Kanzaki et al., 2025).

The realization of CDR may be further delayed through the formation of base cation bearing clay minerals. Clay formation has previously been suggested for EW application based on changes in soil water Ge/Si ratios and Si isotopes (Vienne et al., 2024) and also based on Li isotope measurements (Pogge von Strandmann et al., 2022). These measurements indicated basalt induced clay formation, but it remains unclear what type of clays were formed and hence what the effect on inorganic CO_2 removal may be. In the best case for the inorganic CO_2 removal time lag, the formed clays are 1:1 phyllosilicates such as kaolinite that do not sequester base cations. In this case, DIC leaching is only retarded by base cation exchange. Worst case for the inorganic CO_2 removal time lag, the formed

559 secondary minerals bear substantial amounts of base cations such as chlorite or chrysotile. These clays exhibit a
560 log Wr between -12 and -12.5 at neutral pH (Palandri & Kharaka, 2004), so that dissolution within decadal
561 timescales is unlikely (Bullock et al., 2022).
562
563 Although unfavourable for inorganic CO_2 removal, if base cation bearing secondary clay minerals would form, they
564 can increase SOC (Georgiou et al., 2022; Heckman et al., 2022; Steinwidder et al., 2025). Georgiou et al. (2022)
565 refer to base-cation bearing clays (e.g. smectitic or illitic clays) as 'high-activity minerals' due to their higher SOM
566 stabilization capacity compared to secondary minerals that do not contain base cations (i.e., 'low-activity minerals',
567 with a lower CEC such as kaolinite). Both high- and low-activity minerals can adsorb DOC and form mineral-
568 associated organic matter-C (MAOM-C), which is believed to have a relatively high permanence (decades-
569 centuries) in soils (Lavallee et al., 2020). Besides mineral surface however, plant inputs can also limit SOC accrual.
570 In the latter case, SOC stocks can only increase if belowground plant C inputs increase, which could follow from
571 increases in exchangeable bases or pH (Haque et al., 2019; Shamshuddin et al., 2011). Nonetheless, increases in
572 decomposition can also stimulate SOC losses if rock dust increases soil pH (Klemme et al., 2022).
573
574 **4.2 Implications for monitoring inorganic CO_2 removal**
575
576 Different base cation monitoring strategies are possible. A first option is to quantify TA in soil water (Clarkson et
577 al., 2024). A disadvantage is however that soil water samples have to be sampled across the soil depth.
578 Alternatively, TA could be only monitored in top soil, yet then uncertain TA leaching models must be used (Kanzaki
579 et al., 2025). To calibrate TA leaching models, soil measurements in depth profiles could be used.
580
581 A first soil measurement approach is a total cation accounting approach, which quantifies the loss of base cations
582 from top soils (te Pas et al., 2025). However, this approach only focuses on the top soil and fails to account for
583 physical cation transport from top soils due to erosion or vertical feedstock transport via infiltration or bioturbation.
584 Alternatively, in a mobile/immobile tracer element approach (often named 'TiCat' by the EW community), cation
585 losses from amended top soils are quantified along with immobile tracers, which can account for cation losses
586 through bioturbation or erosion (Reershemius et al., 2023). Nonetheless the disadvantage of TiCat is that it does
587 not track potential TA scavenging (e.g. by organic matter or clays) at larger depth. Our potential inorganic CO_2
588 removal estimate will thus differ from a potential inorganic CO_2 removal estimate quantified using a TiCat approach.
589
590 Alternatively, entire depth profiles could be analyzed to spatially calibrate TA leaching models. Analysis of the
591 exchangeable soil pool is already a well-established method in EW research (Beerling et al., 2024; Reershemius et
592 al., 2023; Reynaert et al., 2023; Vienne et al., 2024). Adding also the carbonate, reducible and oxidizable soil pools
593 to the analysis could make base cation mass balancing more complete. These protocols could calibrate predictive

TA leaching models spatially. In addition there is an opportunity to quantify SOC and MAOM-C changes in the same samples, which have recently gained traction in EW research due to their role in stabilizing SOM (Buss et al., 2024; Sokol et al., 2024; Xu et al., 2024). Integration of these measurements can provide more accurate estimates of the climate impact of EW, but should take into account the difference in permanence of inorganic and organic carbon stocks.

However, this monitoring approach involves complexities such as feedstock correction, leaching solution strength and soil heterogeneity. Although correcting for pre-weathered elements was crucial in this study, it assumes perfect mixing based on a silicate-to-soil ratio. This correction was particularly significant for carbonate and reducible soil pools, where for some base cations, over half of the cation increase with basalt amendment originated from feedstock addition and not from weathering (**Fig. S18**). An alternative approach could involve creating time series from sequential extraction data and quantifying base cation changes based on the change in time between multiple measurements taken after rock amendment.

As discussed in the previous section, another key challenge is that the fate of base cations may remain uncertain if strongly bound crystalline organo-minerals (see Lopez-Sangil & Rovira, 2013) form that are unextractable by the Tessier scheme. Such processes may have contributed to the observed decrease in oxidizable elements at larger depth, although this could also be an artefact of the applied extraction procedure. Pogge von Strandmann et al. (2022) proposed substituting the H_2O_2 leaching step of the Tessier scheme with a dilute HCl leach, which is thought to extract clays as well. Alternatively, post-extraction analysis of residual solids using techniques such as XRD or QEMSCAN may be necessary to rigorously assess changes in rock mineralogy (Mason et al., 2022). Although deep soil core sampling and extensive mineralogical analysis are resource-intensive and not feasible for large-scale application, this monitoring strategy could be valuable during the initial adoption of EW in targeted ‘measure-all’ experiments, as reliable TA leaching models require extensive calibration.

5. Conclusions

This study presents a detailed examination of EW and its effectiveness as a climate mitigation technique, revealing both its potentials and limitations. A novel aspect of this work is the in-depth investigation of entire soil profiles for base cations in different soil fractions, paired with soil water TA monitoring. We highlight the value of sequential extractions as a method for monitoring base cations throughout soil profiles for calibrating TA leaching models.

Our findings indicate that basalt-based enhanced weathering may not immediately lead to the inorganic CO_2 removal previously anticipated in projections and IPCC reports (Babiker et al., 2022; Minx et al., 2018). We observed rock weathering without inorganic CO_2 removal; despite the absence of DIC leaching or carbonate precipitation, exchangeable bases increased with higher basalt amendments, demonstrating that rock weathering occurred.

Additionally, we observed a borderline significant but substantial increase in base cations in the reducible topsoil pool with greater basalt application, which may further suppress TA leaching.

As base cation exchange increased with higher basalt amendments, we infer that greater application rates can further delay the release of DIC from soil minerals to surface waters. However, in practice, EW is typically applied at application rates below 30 t ha^{-1}. These lower, more practical rates may also enhance effectiveness of inorganic CO_2 removal by reducing lag times for DIC release. It remains unclear if clays were formed here and whether EW can deliver CDR within the urgent decadal timeframe needed to mitigate climate change. Despite its limitations for short-term inorganic CO_2 removal, the generated secondary minerals and increased CEC could enhance plant productivity and SOC retention in soils, contributing to long-term soil health, fertility, and potentially carbon sequestration beyond inorganic pathways.

Acknowledgements

We thank Anne Cools, Steven Joosen and Anke De Boeck for their assistance with ICP-OES for sequential extraction samples and Anthony De Schutter to characterize basalt using XRD. We thank DURUBAS to provide basalt and provide the XRF material data sheet. We thank Tom Cox for fruitful discussions. We acknowledge the use of Microsoft Copilot to improve the English of this manuscript. This research was supported by the Research Foundation— Flanders (FWO) [1S06325N], 1174925N] and [G000821N] (Biotic controls of the potential of enhanced silicate weathering for land-based climate change mitigation). We also acknowledge support of the UPSURGE project, which has received funding from the European Union's Horizon 2020 research and innovation program under grant agreement No 101003818.

Author contribution

AV: research conceptualization, data gathering, development methodology, data analysis and writing. PF: conceptualized sequential extraction methodology, writing and discussion. JR: research conceptualization, data gathering. TJS: writing and discussion. TR: writing and discussion. RP: data gathering, rock characterization and writing. JH: writing and discussion. HN: development extraction methodology, writing and discussion. MPE: elemental C measurements and proofreading. LS: writing, development methodology and discussion. LB: writing and discussion. SV: supervising research, conceptualization, writing and discussion.

Data and code availability

Data and code used in this manuscript are freely available at: https://zenodo.org/records/15129984

References

Amann, T., & Hartmann, J. (2022). Carbon Accounting for Enhanced Weathering. *Frontiers in Climate*, *4*(May), 1–9. https://doi.org/10.3389/fclim.2022.849948

Amann, T., Hartmann, J., Hellmann, R., Pedrosa, E. T., & Malik, A. (2022). Enhanced weathering potentials—the role of in situ CO2 and grain size distribution. *Frontiers in Climate*, *4*. https://doi.org/10.3389/fclim.2022.929268

Amann, T., Hartmann, J., Struyf, E., De Oliveira Garcia, W., Fischer, E. K., Janssens, I., Meire, P., & Schoelynck, J. (2020). Enhanced Weathering and related element fluxes - A cropland mesocosm approach. *Biogeosciences*, *17*(1), 103–119. https://doi.org/10.5194/bg-17-103-2020

Barker, S. (2013). Dissolution of Deep-Sea Carbonates. In *Encyclopedia of Quaternary Science* (2nd ed., Vol. 2, Issue 2002). Elsevier B.V. https://doi.org/10.1016/B978-0-444-53643-3.00289-2

Beerling, D. J., Epihov, D. Z., Kantola, I. B., Masters, M. D., Reershemius, T., Planavsky, N. J., & Reinhard, C. T. (2024). Enhanced weathering in the US Corn Belt delivers carbon removal with agronomic benefits. *PNAS*,

1–10. https://doi.org/10.1073/pnas.

Brantley, S. L., White, A. F., & Kubicki, J. D. (2008). Kinetics of water-rock interaction. In *Kinetics of Water-Rock Interaction* (Issue January). https://doi.org/10.1007/978-0-387-73563-4

Buckingham, F. L., Henderson, G. M., Holdship, P., & Renforth, P. (2022). Applied Geochemistry Soil core study indicates limited CO 2 removal by enhanced weathering in dry croplands in the UK. *Applied Geochemistry*, *147*(October), 105482. https://doi.org/10.1016/j.apgeochem.2022.105482

Bullock, L. A., Yang, A., & Darton, R. C. (2022). Kinetics-informed global assessment of mine tailings for CO2 removal. *Science of The Total Environment*, *808*, 152111. https://doi.org/10.1016/j.scitotenv.2021.152111

Buss, W., Hasemer, H., Ferguson, S., & Borevitz, J. (2024). Stabilisation of soil organic matter with rock dust partially counteracted by plants. *Global Change Biology*, *30*(1), 1–14. https://doi.org/10.1111/gcb.17052

Clarkson, M. O., Larkin, C. S., Swoboda, P., Reershemius, T., Suhrhoff, T. J., Maesano, C. N., & Campbell, J. S. (2024). A review of measurement for quantification of carbon dioxide removal by enhanced weathering in soil. *Frontiers in Climate*, *6*(June). https://doi.org/10.3389/fclim.2024.1345224

Dietzen, C., Harrison, R., & Michelsen-Correa, S. (2018). Effectiveness of enhanced mineral weathering as a carbon sequestration tool and alternative to agricultural lime: An incubation experiment. *International Journal of Greenhouse Gas Control*, *74*(January), 251–258. https://doi.org/10.1016/j.ijggc.2018.05.007

Dzombak, D. A., & Morel, F. M. M. (1990). *Surface complexation modeling*. John Wiley & Sons (A Wiley-Interscience Publication).

Fuss, S., Lamb, W. F., Callaghan, M. W., Hilaire, J., Creutzig, F., Amann, T., Beringer, T., De Oliveira Garcia, W., Hartmann, J., Khanna, T., Luderer, G., Nemet, G. F., Rogelj, J., Smith, P., Vicente, J. V., Wilcox, J., Del Mar Zamora Dominguez, M., & Minx, J. C. (2018). Negative emissions - Part 2: Costs, potentials and side effects. *Environmental Research Letters*, *13*(6). https://doi.org/10.1088/1748-9326/aabf9f

Gao, Y., Lu, Y., Wu, M., Liang, E., Li, Y., Zhang, D., Yin, Z., Ren, X., Dai, Y., Deng, D., & Chen, J. (2016). Ability to remove Na+ and retain K+ correlates with salt tolerance in two maize inbred lines seedlings. *Frontiers in Plant Science*, *7*(NOVEMBER2016), 1–15. https://doi.org/10.3389/fpls.2016.01716

Georgiou, K., Jackson, R. B., Vindušková, O., Abramoff, R. Z., Ahlström, A., Feng, W., Harden, J. W., Pellegrini, A. F. A., Polley, H. W., Soong, J. L., Riley, W. J., & Torn, M. S. (2022). Global stocks and capacity of mineral-associated soil organic carbon. *Nature Communications*, *13*(1), 1–12. https://doi.org/10.1038/s41467-022-31540-9

Gislason, S. R., & Oelkers, E. H. (2003). Mechanism, rates, and consequences of basaltic glass dissolution: II. An experimental study of the dissolution rates of basaltic glass as a function of pH and temperature. *Geochimica et Cosmochimica Acta*, *67*(20), 3817–3832. https://doi.org/10.1016/S0016-7037(00)00176-5

Gudbrandsson, S., Wolff-Boenisch, D., Gislason, S. R., & Oelkers, E. H. (2011). An experimental study of crystalline basalt dissolution from 2pH11 and temperatures from 5 to 75°C. *Geochimica et Cosmochimica Acta*, *75*(19), 5496–5509. https://doi.org/10.1016/j.gca.2011.06.035

Haque, F., Santos, R. M., & Chiang, Y. W. (2020). Optimizing Inorganic Carbon Sequestration and Crop Yield With Wollastonite Soil Amendment in a Microplot Study. *Frontiers in Plant Science*, *11*(July), 1–12. https://doi.org/10.3389/fpls.2020.01012

Haque, F., Santos, R. M., Dutta, A., Thimmanagari, M., & Chiang, Y. W. (2019). Co-Benefits of Wollastonite Weathering in Agriculture: CO2 Sequestration and Promoted Plant Growth [Research-article]. *ACS Omega*, *4*(1), 1425–1433. https://doi.org/10.1021/acsomega.8b02477

Heckman, K., Hicks Pries, C. E., Lawrence, C. R., Rasmussen, C., Crow, S. E., Hoyt, A. M., von Fromm, S. F., Shi, Z., Stoner, S., McGrath, C., Beem-Miller, J., Berhe, A. A., Blankinship, J. C., Keiluweit, M., Marín-Spiotta, E., Monroe, J. G., Plante, A. F., Schimel, J., Sierra, C. A., … Wagai, R. (2022). Beyond bulk: Density fractions explain heterogeneity in global soil carbon abundance and persistence. *Global Change Biology*, *28*(3), 1178–1196. https://doi.org/10.1111/gcb.16023

Holzer, I. O., Nocco, M. A., & Houlton, B. Z. (2023). Direct evidence for atmospheric carbon dioxide removal via enhanced weathering in cropland soil. *Environmental Research Communications*, *5*(10). https://doi.org/10.1088/2515-7620/acfd89

Janssens, I. A., Roobroeck, D., Sardans, J., Obersteiner, M., Peñuelas, J., Richter, A., Smith, P., Verbruggen, E., & Vicca, S. (2022). *Negative erosion and negative emissions : Combining multiple land-based carbon dioxide removal techniques to rebuild fertile topsoils and enhance food production*.

Kalinichev, A. G., Iskrenova-Tchoukova, E., Ahn, W. Y., Clark, M. M., & Kirkpatrick, R. J. (2011). Effects of Ca 2+

on supramolecular aggregation of natural organic matter in aqueous solutions: A comparison of molecular modeling approaches. *Geoderma*, *169*, 27–32. https://doi.org/10.1016/j.geoderma.2010.09.002

Kanzaki, Y., Planavsky, N. J., Zhang, S., Jordan, J., Suhrhoff, T. J., & Reinhard, C. T. (2025). Soil cation storage is a key control on the carbon removal dynamics of enhanced weathering. *Environmental Research Letters*, *20*(074055).

Katarzyna A. Kowalczyk, Thorben Amann, Jessica Strefler, M.-E., Vorrath, Jens Hartmann, Serena De Marco, Phil Renforth, S., & Foteinis, E. K. (2024). Marine Carbon Dioxide Removal by alkalinization should no longer be overlooked. *Environmental Research Letters*, *December 2016*, 11–14.

Kelland, M. E., Wade, P. W., Lewis, A. L., Taylor, L. L., Sarkar, B., Andrews, M. G., Lomas, M. R., Cotton, T. E. A., Kemp, S. J., James, R. H., Pearce, C. R., Hartley, S. E., Hodson, M. E., Leake, J. R., Banwart, S. A., & Beerling, D. J. (2020). Increased yield and CO2 sequestration potential with the C4 cereal Sorghum bicolor cultivated in basaltic rock dust-amended agricultural soil. *Global Change Biology*, *26*(6), 3658–3676. https://doi.org/10.1111/gcb.15089

Klemme, A., Rixen, T., Müller, M., Notholt, J., & Warneke, T. (2022). Destabilization of carbon in tropical peatlands by enhanced weathering. *Communications Earth and Environment*, *3*(1), 1–9. https://doi.org/10.1038/s43247-022-00544-0

Larkin, C. S., Andrews, M. G., Pearce, C. R., Yeong, K. L., Beerling, D. J., Bellamy, J., Benedick, S., Freckleton, R. P., Goring-harford, H., Sadekar, S., & James, R. H. (2022). Quantification of CO removal in a large-scale enhanced weathering field trial on an oil palm plantation in Sabah , Malaysia. *Frontiers in Climate*.

Lavallee, J. M., Soong, J. L., & Cotrufo, M. F. (2020). Conceptualizing soil organic matter into particulate and mineral-associated forms to address global change in the 21st century. *Global Change Biology*, *26*(1), 261–273. https://doi.org/10.1111/gcb.14859

Lefebvre, D., Goglio, P., Williams, A., Manning, D. A. C., Carlos, A., Azevedo, D., Bergmann, M., Meersmans, J., & Smith, P. (2019). Assessing the potential of soil carbonation and enhanced weathering through Life Cycle Assessment : A case study for Sao Paulo State , Brazil. *Journal of Cleaner Production*, *233*, 468–481. https://doi.org/10.1016/j.jclepro.2019.06.099

Lopez-Sangil, L., & Rovira, P. (2013). Sequential chemical extractions of the mineral-associated soil organic matter: An integrated approach for the fractionation of organo-mineral complexes. *Soil Biology and Biochemistry*, *62*, 57–67. https://doi.org/10.1016/j.soilbio.2013.03.004

Manning, D. A. C., Renforth, P., Lopez-Capel, E., Robertson, S., & Ghazireh, N. (2013). Carbonate precipitation in artificial soils produced from basaltic quarry fines and composts: An opportunity for passive carbon sequestration. *International Journal of Greenhouse Gas Control*, *17*, 309–317. https://doi.org/10.1016/j.ijggc.2013.05.012

Mason, J., Lin, E., Grono, E., & Denham, T. (2022). QEMSCAN® analysis of clay-rich stratigraphy associated with early agricultural contexts at Kuk Swamp, Papua New Guinea. *Journal of Archaeological Science: Reports*, *42*(February), 103356. https://doi.org/10.1016/j.jasrep.2022.103356

Matylda Hermanska , Martin J. Voigt, Chiara Marieni, Julien Declercq, E. O. (2022). *A comprehensive and internally consistent mineral dissolution rate database : Part I : Primary silicate minerals and glasses*. *597*(July 2021). https://doi.org/10.1016/j.chemgeo.2022.120807

McDermott, F., Bryson, M., Magee, R., & van Acken, D. (2024). Enhanced weathering for CO2 removal using carbonate-rich crushed returned concrete; a pilot study from SE Ireland. *Applied Geochemistry*, *169*(June), 106056. https://doi.org/10.1016/j.apgeochem.2024.106056

Minx, J. C., Lamb, W. F., Callaghan, M. W., Fuss, S., Hilaire, J., Creutzig, F., Amann, T., Beringer, T., De Oliveira Garcia, W., Hartmann, J., Khanna, T., Lenzi, D., Luderer, G., Nemet, G. F., Rogelj, J., Smith, P., Vicente Vicente, J. L., Wilcox, J., & Del Mar Zamora Dominguez, M. (2018). Negative emissions - Part 1: Research landscape and synthesis. *Environmental Research Letters*, *13*(6). https://doi.org/10.1088/1748-9326/aabf9b

Morse, J. W., Arvidson, R. S., & Lüttge, A. (2007). Calcium carbonate formation and dissolution. *Chemical Reviews*, *107*(2), 342–381. https://doi.org/10.1021/cr050358j

Navarre-Sitchler, A., & Brantley, S. (2007). Basalt weathering across scales. *Earth and Planetary Science Letters*, *261*(1–2), 321–334. https://doi.org/10.1016/j.epsl.2007.07.010

Niron, H., Vienne, A., Frings, P., Poetra, R., & Vicca, S. (2024). Exploring the synergy of enhanced weathering and Bacillus subtilis: A promising strategy for sustainable agriculture. *Global Change Biology*, *30*(9), 1–18. https://doi.org/10.1111/gcb.17511

Öquist, M. G., Wallin, M., Seibert, J., Bishop, K., & Laudon, H. (2009). Dissolved Inorganic Carbon Export Across

the Soil / Stream Interface and Its Fate in a Boreal Headwater Stream. *Environmental Science & Technology*, *43*(19), 7364–7369.

Palandri, J. L., & Kharaka, Y. K. (2004). A compilation of rate parameters of water-mineral interaction kinetics for application to geochemical modeling. *USGS Open File Report*, *2004–1068*, 71. http://www.dtic.mil/cgi-bin/GetTRDoc?Location=U2&doc=GetTRDoc.pdf&AD=ADA440035

Poeplau, C., Don, A., Six, J., Kaiser, M., Benbi, D., Chenu, C., Cotrufo, M. F., Derrien, D., Gioacchini, P., Grand, S., Gregorich, E., Griepentrog, M., Gunina, A., Haddix, M., Kuzyakov, Y., Kühnel, A., Macdonald, L. M., Soong, J., Trigalet, S., … Nieder, R. (2018). Isolating organic carbon fractions with varying turnover rates in temperate agricultural soils – A comprehensive method comparison. *Soil Biology and Biochemistry*, *125*(April), 10–26. https://doi.org/10.1016/j.soilbio.2018.06.025

Pogge von Strandmann, P. A. E., Liu, X., Liu, C. Y., Wilson, D. J., Hammond, S. J., Tarbuck, G., Aristilde, L., Krause, A. J., & Fraser, W. T. (2022). Lithium isotope behaviour during basalt weathering experiments amended with organic acids. *Geochimica et Cosmochimica Acta*, *328*, 37–57. https://doi.org/10.1016/j.gca.2022.04.032

Power, I. M., Hatten, V. N. J., Guo, M., Rausis, K., & Klyn-hesselink, H. (2025). Are enhanced rock weathering rates overestimated ? A few geochemical and mineralogical pitfalls. *Frontiers in Climate*, *6*(January), 1–9. https://doi.org/10.3389/fclim.2024.1510747

Reershemius, T., Kelland, M. E., Jordan, J. S., Davis, I. R., D'Ascanio, R., Kalderon-Asael, B., Asael, D., Suhrhoff, T. J., Epihov, D. Z., Beerling, D. J., Reinhard, C. T., & Planavsky, N. J. (2023). Initial Validation of a Soil-Based Mass-Balance Approach for Empirical Monitoring of Enhanced Rock Weathering Rates. *Environmental Science and Technology*, *57*(48), 19497–19507. https://doi.org/10.1021/acs.est.3c03609

Renforth, P. (2012). The potential of enhanced weathering in the UK. *International Journal of Greenhouse Gas Control*, *10*, 229–243. https://doi.org/10.1016/j.ijggc.2012.06.011

Renforth, Phil. (2019). The negative emission potential of alkaline materials. *Nature Communications*, *10*(1). https://doi.org/10.1038/s41467-019-09475-5

Renforth, Phil, & Henderson, G. (2017). Assessing ocean alkalinity for carbon sequestration. *Reviews of Geophysics*, *55*(3), 636–674. https://doi.org/10.1002/2016RG000533

Reynaert, S., Vienne, A., De Boeck, H. J., D'Hose, T., Janssens, I., Nijs, I., Portillo-Estrada, M., Verbruggen, E., Vicca, S., & Poblador, S. (2023). Basalt addition improves the performance of young grassland monocultures under more persistent weather featuring longer dry and wet spells. *Agricultural and Forest Meteorology*, *340*(July), 109610. https://doi.org/10.1016/j.agrformet.2023.109610

Rijnders, J., Vienne, A., & Vicca, S. (2025). Effects of basalt, concrete fines, and steel slag on maize growth and toxic trace element accumulation in an enhanced weathering experiment. *Biogeosciences*, *22*(12), 2803–2829. https://doi.org/10.5194/bg-22-2803-2025

Rowley, M. C., Grand, S., & Verrecchia, É. P. (2018). Calcium-mediated stabilisation of soil organic carbon. *Biogeochemistry*, *137*(1–2), 27–49. https://doi.org/10.1007/s10533-017-0410-1

Ryan, P. C., Hillier, S., & Wall, A. J. (2008). Stepwise effects of the BCR sequential chemical extraction procedure on dissolution and metal release from common ferromagnesian clay minerals: A combined solution chemistry and X-ray powder diffraction study. *Science of the Total Environment*, *407*(1), 603–614. https://doi.org/10.1016/j.scitotenv.2008.09.019

Schindlbacher, A., Beck, K., Holzheu, S., & Borken, W. (2019). Inorganic Carbon Leaching From a Warmed and Irrigated Carbonate Forest Soil. *Frontiers in Forest and Global Change*, *2*(August), 1–13. https://doi.org/10.3389/ffgc.2019.00040

Shamshuddin, J., Anda, M., Fauziah, C. I., & Omar, S. S. R. (2011). Growth of cocoa planted on highly weathered soil as affected by application of basalt and/or compost. *Communications in Soil Science and Plant Analysis*, *42*(22), 2751–2766. https://doi.org/10.1080/00103624.2011.622822

Smith, P., Davis, S. J., Creutzig, F., Fuss, S., Minx, J., Gabrielle, B., Kato, E., Jackson, R. B., Cowie, A., Kriegler, E., Van Vuuren, D. P., Rogelj, J., Ciais, P., Milne, J., Canadell, J. G., McCollum, D., Peters, G., Andrew, R., Krey, V., … Yongsung, C. (2016). Biophysical and economic limits to negative CO2 emissions. *Nature Climate Change*, *6*(1), 42–50. https://doi.org/10.1038/nclimate2870

Sokol, N. W., Sohng, J., Moreland, K., Slessarev, E., Goertzen, H., Schmidt, R., Samaddar, S., Holzer, I., Almaraz, M., Geoghegan, E., Houlton, B., Montañez, I., Pett-Ridge, J., & Scow, K. (2024). Reduced accrual of mineral-associated organic matter after two years of enhanced rock weathering in cropland soils, though no net losses of soil organic carbon. *Biogeochemistry Letters*, *167*(8), 989–1005. https://doi.org/10.1007/s10533-024-01160-0

Steinwidder, L., Boito, L., Frings, P. J., Niron, H., Rijnders, J., de Schutter, A., Vienne, A., & Vicca, S. (2025). Beyond Inorganic C: Soil Organic C as a Key Pathway for Carbon Sequestration in Enhanced Weathering. *Global Change Biology*, *31*(7). https://doi.org/10.1111/gcb.70340

Steinwidder, L., Boito, L., Frings, P., Niron, H., Rijnders, J., De Schutter, A., Vienne, A., & Vicca, S. (2025). Beyond inorganic carbon : Soil organic carbon as key pathway for carbon sequestration in Enhanced Weathering. *Global Change Biology*.

Strefler, J., Amann, T., Bauer, N., Kriegler, E., & Hartmann, J. (2018). Potential and costs of carbon dioxide removal by enhanced weathering of rocks. *Environmental Research Letters*, *13*(3). https://doi.org/10.1088/1748-9326/aaa9c4

Suarez, D. L., & Grieve, C. M. (1988). Predicting cation ratios in corn from saline solution composition. *Journal of Experimental Botany*, *39*(5), 605–612. https://doi.org/10.1093/jxb/39.5.605

Swoboda, P., Döring, T. F., & Hamer, M. (2021). Remineralizing soils? The agricultural usage of silicate rock powders: A review. *Science of the Total Environment*, *807*(150976), 18. https://doi.org/10.1016/j.scitotenv.2021.150976

Takaya, Y., Wu, M., & Kato, Y. (2019). Unique environmental conditions required for dawsonite formation: Implications from dawsonite synthesis experiments under alkaline conditions. *ACS Earth and Space Chemistry*, *3*(2), 285–294. https://doi.org/10.1021/acsearthspacechem.8b00121

Taylor, L., Driscoll, C., Groffman, P., Rau, G., Blum, J., & Beerling, D. (2021). Increased carbon capture by a silicate-treated forested watershed affected by acid deposition. *Biogeosciences Discussions*, 1–29. https://doi.org/10.5194/bg-2020-288

te Pas, E. E. E. M., Chang, E., Marklein, A. R., Comans, R. N. J., & Hagens, M. (2025). Accounting for retarded weathering products in comparing methods for quantifying carbon dioxide removal in a short-term enhanced weathering study. *Frontiers in Climate*, *2029*(February), 1–10. https://doi.org/10.3389/fclim.2024.1524998

te Pas, E. E. E. M., Hagens, M., & Comans, R. N. J. (2023). Assessment of the enhanced weathering potential of different silicate minerals to improve soil quality and sequester CO2. *Frontiers in Climate*, *4*. https://doi.org/10.3389/fclim.2022.954064

Tessier, A., Campbell, P. G. C., & Bisson, M. (1979). Sequential Extraction Procedure for the Speciation of Particulate Trace Metals. *Analytical Chemistry*, *51*(7), 844–851. https://doi.org/10.1021/ac50043a017

Van Bemmelen, J. (1890). Über Die Bestimmung Des Wassers, Des Humus, Des Schwefels, Der in Den Colloïdalen Silikaten Gebundenen Kieselsäure, Des Mangans U. S. W. Im Ackerboden. *Die Landwirthschaftlichen Versuchs-Stationen*, *37*, 279–290.

Van Der Bauwhede, R., Muys, B., Vancampenhout, K., & Smolders, E. (2024). Geoderma Accelerated weathering of silicate rock dusts predicts the slow-release liming in soils depending on rock mineralogy , soil acidity , and test methodology. *Geoderma*, *441*(November 2023), 116734. https://doi.org/10.1016/j.geoderma.2023.116734

Van Straaten, P. (2006). Farming with rocks and minerals: Challenges and opportunities. *Anais Da Academia Brasileira de Ciencias*, *78*(4), 731–747. https://doi.org/10.1590/S0001-37652006000400009

Vienne, A., Frings, P., Poblador, S., Steinwidder, L., Rijnders, J., Schoelynck, J., Vinduskova, O., & Vicca, S. (2024). Earthworms in an enhanced weathering mesocosm experiment : Effects on soil carbon sequestration , base cation exchange and soil CO 2 efflux. *Soil Biology and Biochemistry*, *199*(June), 109596. https://doi.org/10.1016/j.soilbio.2024.109596

Vienne, A., Poblador, S., Portillo-estrada, M., Hartmann, J., Ijiehon, S., Wade, P., & Vicca, S. (2022). Enhanced Weathering Using Basalt Rock Powder : Carbon Sequestration , Co-benefits and Risks in a Mesocosm Study With Solanum tuberosum. *Frontiers in Climate*, *4*(May), 1–14. https://doi.org/10.3389/fclim.2022.869456

Wolf-Gladrow, D. A., Zeebe, R. E., Klaas, C., Körtzinger, A., & Dickson, A. G. (2007). Total alkalinity: The explicit conservative expression and its application to biogeochemical processes. *Marine Chemistry*, *106*(1-2 SPEC. ISS.), 287–300. https://doi.org/10.1016/j.marchem.2007.01.006

Xu, T., Yuan, Z., Vicca, S., Goll, D. S., Li, G., Lin, L., Chen, H., Bi, B., Chen, Q., Li, C., Wang, X., Wang, C., Hao, Z., Fang, Y., & Beerling, D. J. (2024). Enhanced silicate weathering accelerates forest carbon sequestration by stimulating the soil mineral carbon pump. *Global Change Biology*, *30*(8), 1–17. https://doi.org/10.1111/gcb.17464

Zhang, S., Planavsky, N. J., Katchinoff, J., Raymond, P. A., Kanzaki, Y., Reershemius, T., & Reinhard, C. T. (2022). River chemistry constraints on the carbon capture potential of surficial enhanced rock weathering. *Limnology and Oceanography*, *67*(S2), S148–S157. https://doi.org/10.1002/lno.12244

886